2014 American Control Conference (ACC)
June 4-6, 2014. Portland, Oregon, USA

Optimal Power Management for a Series Hybrid Electric Vehicle Cognizant of Battery Mechanical Effects

Youngki Kim*, Shankar Mohan, Nassim A. Samad, Jason B. Siegel and Anna G. Stefanopoulou

Abstract— **This paper presents an optimal power management strategy for a series hybrid electric vehicle (SHEV) with the consideration of battery bulk mechanical stress. The relation between mechanical stress and state-of-charge (SOC) is characterized first. Then, this relation is used to penalize the battery usage leading to capacity fade due to particle fracture in the negative electrode. The optimal power management strategy is found using Dynamic Programming (DP) not only for maximizing fuel economy but also for minimizing the battery cumulative bulk mechanical stress. DP results suggest that battery SOC needs to be regulated around a lower value for prolonged battery life. Moreover, it is found that the cumulative bulk mechanical stress can be significantly reduced at a small expense of fuel economy.**

I. INTRODUCTION

Lithium-ion (Li-ion) batteries have high energy/power density and broad operating temperature ranges capable of supporting vehicle electrification [1], [2]. This paper concerns itself with electrified vehicles that are propelled by hybrid powertrain systems. Supervisory controllers to manage energy or power flow among hybrid systems have been studied to fully exploit the potential of electrified vehicles [3]–[5].

Battery longevity or health in terms of cycle-life is one of the significant factors regarding marketability of electrified vehicles[1]. In recent times, a new breed of supervisor controllers that are conscious of the health of Li-ion cells have been proposed [6]–[9]. The health of Li-ion batteries, a pseudo indicator of the age of cells, is typically judged by monitoring internal resistance and capacity. Measurable changes in internal resistance and capacity are a result of electro-chemical/mechanical degradation [10], [11]. In particular, Ebbesen et al. introduce a state-of-health (SOH) perceptive energy management strategy for HEVs wherein a throughput based SOH model is used to capture battery capacity fade [7]. Moura et al. consider resistive film growth in the negative electrode while developing a framework to formulate a multi-objective optimal power management problem for PHEVs [8]. The model for the resistance growth was supported by observations on the electrochemical phenomena in cells.

From an electrochemical perspective, the increase in resistance can be attributed to the occurrence of side reactions between the electrodes and the electrolyte; the formation of Solid Electrolyte Interface (SEI) at the anode; and the loss of contact with the binder and the collectors. The formation of the SEI is typically accompanied by a reduction in capacity as a result of the reduction in available Li-ions.

Aging related electrochemical phenomena are inherently coupled with mechanical effects. Recently, several studies have been conducted to investigate battery ageing mechanisms. Aside from electrode bending which could cause loss of contact, lithium de/intercalation into the graphite electrode results in its expanding/contracting; this results in particles cracking and the formation of SEI [12], [13]. Given its influence on the health of cells and the chain of causation, it is imperative that aging related mechanical effects be considered in the design of supervisory automotive controllers.

In this paper, we investigate the optimal power management for a SHEV by accounting for the bulk mechanical stress. In the greater scheme of effectively incorporating mechanical information into the design of controllers, as a first step, the accumulation of mechanical stress is considered as an indirect indicator of accelerated capacity fade. Experiments are conducted to characterize the relation between mechanical stress, temperature and battery SOC. This characterized relation is used to penalize the battery usage in an effort to minimize capacity fade. To objectively study the impact of the penalty on the operation of the hybrid powertrain, Dynamic Programming (DP) is used to solve the off-line optimal power management problem.

This paper is organized as follows. Section II describes the experimental set-up and design utilized to develop a quasi-static model to predict the battery bulk stress. In Section III, the optimal power management problem is formulated to minimize fuel consumption and the battery cumulative bulk mechanical stress (BCBMS). Optimal solutions and the tradeoff between fuel consumption and battery cyclelife are discussed in Section IV. Finally, conclusions are drawn in Section V.

II. MODEL STRUCTURE

The model for battery mechanical stress is the core to the development of the proposed power management strategy. To begin with, it is important to understand the influence of mechanical stress on performance degradation of Li-ion batteries. This section focuses on the characterization of mechanical stress of the battery including a carefully designed experimental set-up. Additionally, the powertrain model for the SHEV is also briefly described.

* Corresponding author: youngki@umich.edu
The authors are with University of Michigan, Ann Arbor, MI, 48109, USA

[1]Automakers such as Nissan and Chevrolet warrant their battery packs equipped in Leaf and Volt respectively for 8 years or 100,000 miles.

978-1-4799-3274-0/$31.00 ©2014 AACC

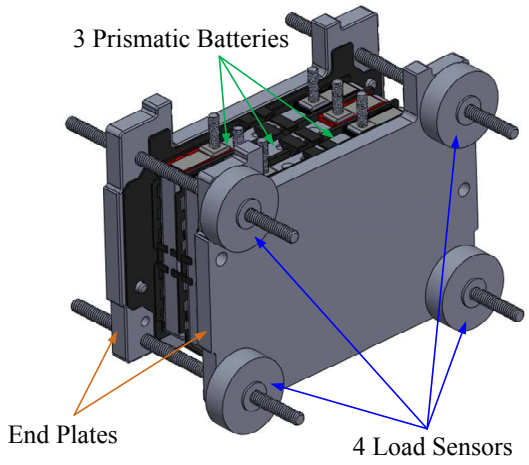

Fig. 1. Illustration of the fixture for mechanical stress measurement

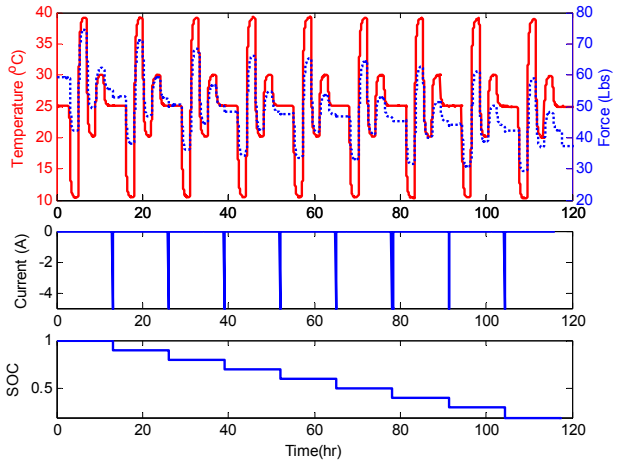

Fig. 2. Experimental setup to characterize mechanical stress of the battery: temperature and force (top); current (middle); and SOC (bottom)

A. Mechanical Effects Overview

In the negative electrode, the particle breakdown results in the formation of SEI, loss of available lithium and increased resistance. Kostecki and McLarnon observed in [14] that structural disordering of graphite particle near the separator in the negative electrode and suggested that the structural degradation leads to an increased resistivity. In [15], Christensen and Newman suggested that this structural degradation is led by the high stress during Lithium intercalation/deintercalation.

The positive electrode materials also suffer from the mechanical stress induced by the volumetric change during cycling. In [16], Cho et al. observed that the capacity fade is related to large lattice expansion of the positive electrode material. The authors have suggested that prolonged battery life can be achieved by suppressing expansion with the encapsulation of positive electrode material.

Mechanical stress or expansion at the electrode level is not easy to measure. Siegel et al. used Neutron Imaging, an *in situ* measurement technique, to quantify expansion at the electrode sandwich layer-level (expansion between two aluminum current collectors) in [17], wherein they also observed correlated capacity loss during cycling of lithium iron phosphate pouch cells at elevated potential. Cannarella and Arnold studied a stack level mechanical stress and and its influence on capacity fade [18]. By performing tests on pouch cells, the authors use empirical evidence to conclude that the capacity fade is accelerated when under high bulk stress. In this paper, we adopt a similar strategy to measure the bulk mechanical stress by retrofitting a pack with load cells as elaborated in the next subsection.

B. Mechanical Bulk Stress Model

As shown in Fig. 1, a 3-Cell Li-ion battery fixture was manufactured with the purpose of measuring the mechanical force resulting from mechanical bulk stresses, and temperatures at the surface of the Li-ion cell. The Li-ion battery is a Lithium-Nickel-Manganese-Cobalt-Oxide (NMC) prismatic type cell with dimensions of 120 mm $\times$ 85 mm $\times$ 12.7 mm and a 5Ah capacity. Three cells are clamped down between two garolite end plates held together with nuts and bolts to provide a smooth compressing surface. Four Omega load sensors LC8150-250-100 each with a force rating of 100 lbs, were bolted at the four corners of one garolite end plate. The whole fixture was placed in a Cincinnati Sub-Zero ZPHS16-3.5-SCT/AC environmental chamber to allow for temperature regulation.

The experimental procedure for characterizing bulk stress is shown in Fig. 2. The battery was fully charged at a rate of C/20[2] at 25°C using a Constant Current Constant Voltage protocol with a cutoff current rate of C/100. The temperature in the thermal chamber is controlled as shown in Fig. 2(a). The battery is allowed to rest for two hours at each temperature to equilibrate. To change the SOC of the battery by 10%, a 1C current is applied to the battery for six minutes at 25°C. Each step change in SOC is followed by two hours of rest for charge equilibrium. The battery bulk stress is calculated as

$$BS = \frac{\sum \text{Force}}{\text{Area}}. \quad (1)$$

Figure 4 shows the measured battery force as a function of SOC and temperature. It is observed that the battery force increases monotonically with increasing SOC and temperature respectively. The volumetric changes in the positive and negative electrodes cannot be distinguished from the measured force signal since the only bulk change is measured. However, the volumetric change of the positive electrode material, NMC, is much lower than that of the negative electrode material, graphite as summarized in Table I. Therefore, it is reasonable to assume that this measured force is attributed to swelling in the negative electrode. It is also

[2]A 1C current corresponds to the magnitude of current that discharges/charges the battery completely in one hour.

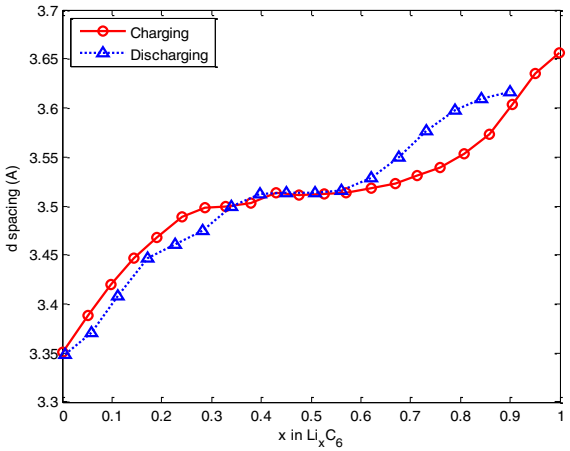

Fig. 3. The average graphene interlayer spacing during the lithium de/intercalation [20]

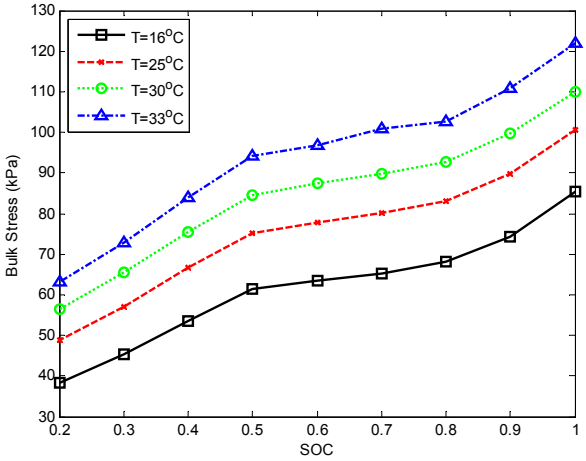

Fig. 4. Measured bulk mechanical stress as a function of SOC and temperature

found that the overall shape of the measured force is similar to the measured stress of the negative electrode reported in [20] (Figure 3).

The rate of capacity fade is accelerated when operating under high stress [18]. Consequently, the normalized nonlinear function illustrated in Fig. 4 will be used as a cost function to account for battery performance degradation in developing a supervisory controller for HEVs in Section III.

In the following subsection, the relation between bulk level mechanical stress is characterized through a carefully designed experiment.

C. Series Hybrid Electric Powertrain Model

The engine/generator is modeled by using a quasi-static nonlinear map representing the relationship between power and fuel rate. This model is suitable under the assumption that transients of the engine and generator are much faster than the system-level energy flow dynamics [3]. Similarly, the efficiency and maximum torque maps are used to model the motor.

To model the SOC dynamics of the battery, a single state equivalent circuit model is considered as following:

$$\frac{d\text{SOC}}{dt} = -\frac{I}{C_b}, \tag{2}$$

$$I = \frac{V_{oc}(\text{SOC}) - \sqrt{(V_{oc}(\text{SOC}))^2 - 4R_s(\text{SOC})P_b}}{2R_s(\text{SOC})}, \tag{3}$$

$$V_t = V_{oc}(\text{SOC}) - IR_s(\text{SOC}), \tag{4}$$

where V_{oc}, R_s and C_b are the open circuit voltage, internal resistance and capacity of the battery. Specifically, V_{oc} and R_s are tabulated in lookup tables as functions of SOC as shown in Fig. 5. The battery current, power and terminal voltage are denoted by I, P_b and V_t, respectively.

For the purpose of formulating an optimal control problem, a discrete-time system will be used instead of a continuous-time system in the following section.

TABLE I
VOLUMETRIC STRAIN CHANGE OF VARIOUS COMPOUNDS [19]

Electrode	Compound	Value [%]
Positive	$LiCoO_2$	+1.9
	$LiNiO_2$	-2.8
	$LiMn_2O_4$	-7.3
	$LiNi_{1/3}Mn_{1/3}Co_{1/3}O_2^\star$	+2.44
Negative	Graphite C_6	+12.8

$\star$ is the most similar to the positive electrode material in this study

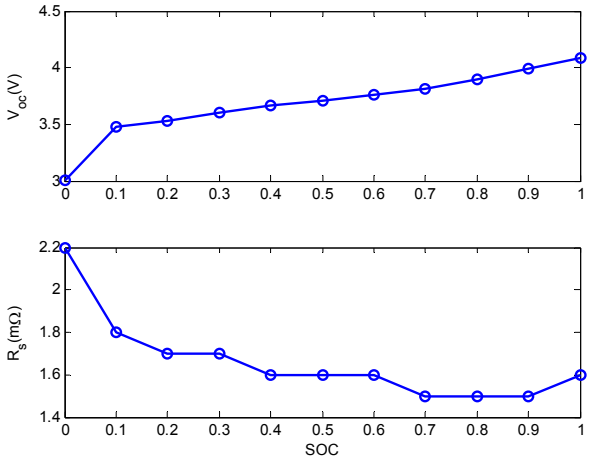

Fig. 5. Open circuit voltage and internal resistance as a function of SOC at 25°C

III. Optimal Power Management

The optimal problem for power management in an SHEV is formulated to minimize the cost function J over a finite horizon a length of N as following:

$$\min_{u_k} \quad \left\{ J = \sum_{k=0}^{N-1} g(x_k, u_k, w_k) \right\} \tag{5}$$

$$\text{Subject to} \quad -0.2 \leq \text{SOC}_k - \text{SOC}_0 \leq 0.2 \tag{6}$$

$$\text{SOC}_0 = \text{SOC}_N \tag{7}$$

$$-20 \leq u_k \leq 20 \tag{8}$$

$$0 \leq P_{eg,k} \leq 58 \tag{9}$$

$$-11 \leq \Delta P_{eg,k} \leq 11 \tag{10}$$

where x_k, u_k and w_k are states, inputs and disturbances, respectively and are defined as

$$x_k = [\text{SOC}_k \; P_{eg,k}]^T, u_k = P_{b,k}, w_k = P_{req,k}$$

where $P_{eg,k} = w_k - u_k$ and $P_{req,k}$ are the engine/generator power and the power request in kW given by a driving cycle for a vehicle, respectively.

The overall operation is enforced to be charge-sustaining to enable fair comparison of fuel economy amongst different control parameters. From [21], considering pulse power capability, the deviation of SOC around nominal SOC is restricted to 0.2.

The state $P_{eg,k}$ is introduced to consider the power rate of the engine/generator $\Delta P_{eg,k}$ as a constraint, enabling smooth engine operations. Smooth transients of the engine prevent deviations from the optimal operation line. The maximum allowable power rates are adopted from [22].

The instantaneous cost function g is the weighted sum of the normalized fuel consumption FC_{norm}, the normalized bulk stress BS_{norm} and the normalized battery current $|I_{norm}|$ (Figure 6) given by

$$g = \vartheta_1 FC_{norm} + \vartheta_2 BS_{norm} + \vartheta_3 |I_{norm}| \tag{11}$$

where nonnegative weighting factors ϑ's satisfy an equality constraint: $\vartheta_1 + \vartheta_2 + \vartheta_3 = 1$ and $\vartheta_i \geq 0 \; i = 1, 2, 3$. These normalized penalties are obtained by scaling fuel consumption, bulk stress and current to lie within zero and one. The normalized battery mechanical stress BS_{norm} is related to the capacity fade due to particle fracture in the negative electrode. As provided in [18], the battery cumulative bulk mechanical stress (BCBMS) leads to a performance degradation with higher stress resulting in higher rates of capacity fade. Since a detailed capacity fade model is under development, the linear relation between the capacity fade and BCBMS is considered as a first step. The last term in Eq. (11) $|I_{norm}|$ is used to adopt an ampere-hour (AH) processed model assuming that capacity fade is proportional to the integrated number of lithium ions only.

To solve the optimal problem, Dynamic Programming (DP) is used in this study. DP is a powerful numerical tool to determine optimal control policies or trajectories explicitly using the Bellman's optimality principle which is a sufficient condition for the optimality. Therefore, the DP solution is the global optimum even for nonlinear systems with constraints [23]. The MATLAB-based DPM function developed by Sundström and Guzzella [24] was used to numerically solve the optimization problem.

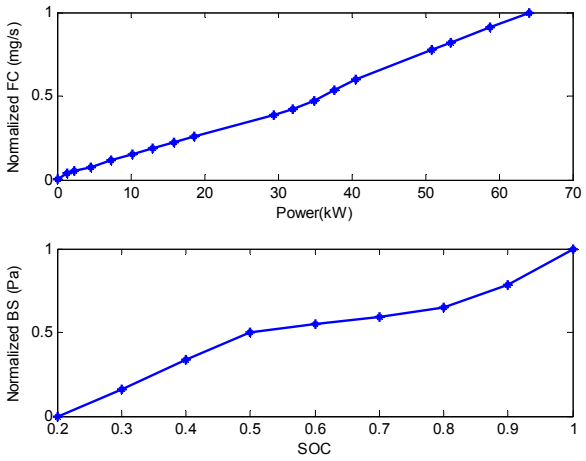

Fig. 6. The normalized fuel consumption by the engine/generator and the mechanical bulk stress of the battery

IV. Results and Discussion

To analyze the tradeoff between fuel economy and battery degradation, the weighting factors ϑ is parametrically varied from zero to one. Moreover, four different SOC set points are considered to investigate their influence on objectives, i.e. $\text{SOC}_0 \in \{0.4, 0.5, 0.6, 0.7\}$. To isolate the influence of penalizing Ah-processed on fuel economy, the case ($\vartheta_3 = 0$) is studied.

For the simulation, the US06 Supplemental Federal Test Procedure (SFTP) cycle is selected since this cycle is aggressive compared to other federal cycles such as the Urban Dynamometer Driving Schedule (UDDS) and the highway fuel economy test (HWFET). The US06 cycle has the average and maximum speeds of 48.4 mph (77.9 kph) and 80.3 mph (129.2 kph) respectively as well as high acceleration/deceleration driving behavior. The specifications of the SHEV under consideration are provided in Table II.

From Fig. 5 and 6, it is expected that fuel economy and BCBMS are in conflict with one another. The best battery operation in terms of minimizing bulk mechanical stress is obtained when SOC set point is 0.4, which is explained by the fact that nonlinear stress curve is monotonically increasing with SOC (Figure 4). This result is corroborated

TABLE II
Series Hybrid Electric Vehicle Specifications

Mass [kg]	Frontal area [m^2]	Drag coeff. [−]	Rolling resistance [−]
1715	2.22	0.281	0.01

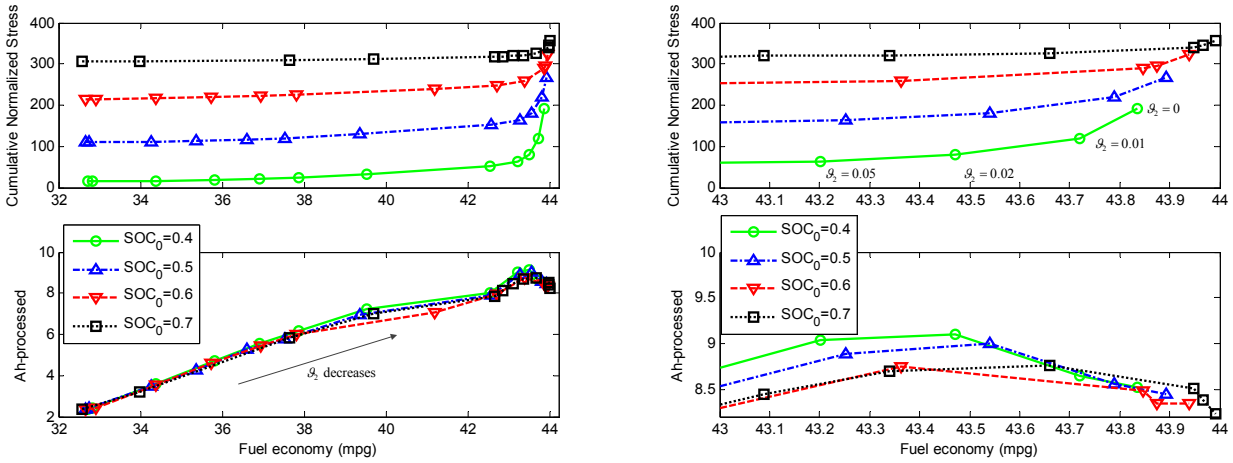

(a) (b)

Fig. 7. (a) Pareto-curve of fuel economy vs. the cumulative mechanical bulk stress and corresponding Ah-processed over various weighting factors at different SOC set points (b) zoom view

by experimental results provided in [25] where the authors have observed that battery operations at high SOC (or high voltage) exhibit fast ageing compared to battery operations at low SOC.

On the other hand, the best fuel economy is achieved when SOC is 0.7. This high fuel economy can be attributed to the high open circuit voltage and low internal resistance at high SOC as shown in Fig. 5. For the same power supplied from the pack, lower current is drawn at higher SOC since the open circuit voltage is higher. Power loss is the product of resistance and the square of current; and is lower when the battery operates at higher SOC. Figures 7(a) and 7(b) highlight the said tradeoff between fuel economy and BCBMS for four different SOC set points.

Unlike the tradeoff between fuel economy and BCBMS, the relationship between Ah-processed and BCBMS needs interpretation. As the penalty on BCBMS is increased, it is anticipated that the transient nominal SOC is closer to the lower bound of SOC operating window and battery utilization reduces. However, for smaller values of ϑ_2, it is observed that Ah-processed increases as shown in Fig. 7(b). To better understand this phenomena, two solutions from the Pareto curve ($\vartheta_2 = 0$ and $\vartheta_2 = 0.01$ at SOC_0=0.4) are compared as shown in Fig. 8. The optimal solution with a small penalty on bulk mechanical stress selectively prefers the battery for the vehicle propulsion more in the initial and final time periods than when $\vartheta_2 = 0$, resulting in lower operating SOC and lower bulk mechanical stress. This result suggests that batteries may degrade due to increased usage in spite of penalizing bulk mechanical stress. In particular, by penalizing battery usage with the knowledge of mechanical stress with $\vartheta_2 = 0.01$, BCBMS can be reduced by 38.5% with deterioration of fuel economy and Ah-processed about 0.3% and 1.48%, respectively. Thus, fuel economy has to be sacrificed to maintain the battery usage in the same level while minimizing BCBMS.

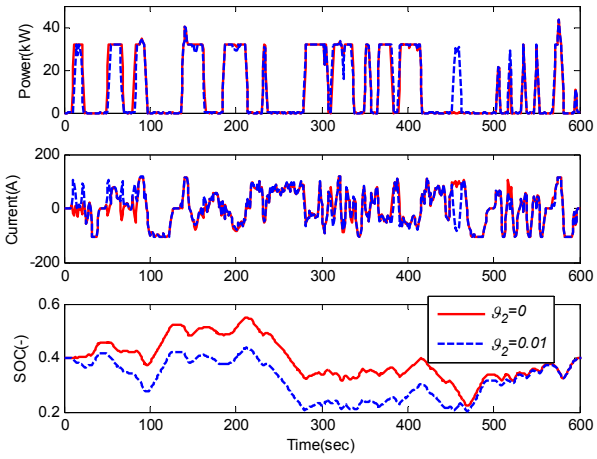

Fig. 8. Simulated transient behaviors under two optimal power management strategies: ϑ_2=0 & ϑ_2=0.01 at SOC_0=0.4

V. CONCLUSION

An optimal power management strategy is developed to account for battery bulk mechanical stress effects as an indicator of battery performance degradation as well as fuel economy in SHEVs. The impact on battery health of HEV operations is implicitly gauged by using two concepts. One is the well-known and widely-accepted Ah-processed and the other is the accumulation of mechanical stress, a newly proposed concept in power management studies. Battery bulk mechanical stress is modeled using a quasi-static nonlinear map through a carefully designed experiment. Then, the optimal power management control problem is formulated and is numerically solved using DP.

It is observed that when operating at a high SOC, both fuel economy and BCBMS increase. On the other hand, both objectives decrease at lower SOC set point. However, Ah-processes is almost independent of SOC set point. DP results

show that BCBMS can be significantly reduced at a small expense of fuel economy.

In a first step towards incorporating battery mechanical effects in power management strategies, this work utilized a quasi-static relation between SOC and bulk mechanical stress. This framework can be further extended by including a dynamic model for battery swelling and by incorporating electrode phase transition information. A future work will aspire to provide experimental validation results based on the framework proposed in this paper and develop a real-time implementable strategy by applying Pontryagin's Maximum (or Minimum) Principle or Model Predictive Control.

REFERENCES

[1] R. Huggins, *Advanced Batteries: Materials Science Aspects, first edition*. Springer, 2008.

[2] Z. Rao and S. Wang, "A review of power battery thermal energy management," *Renewable and Sustainable Energy Reviews*, vol. 15, no. 9, pp. 4554–4571, 2011.

[3] C.-C. Lin, H. Peng, J. Grizzle, and J.-M. Kang, "Power management strategy for a parallel hybrid electric truck," *Control Systems Technology, IEEE Transactions on*, vol. 11, no. 6, pp. 839–849, 2003.

[4] J. Liu, J. Hagena, H. Peng, and Z. S. Filipi, "Engine-in-the-loop study of the stochastic dynamic programming optimal control design for a hybrid electric HMMWV," *International Journal of Heavy Vehicle Systems*, vol. 15, no. 2-4, pp. 309–326, 2008.

[5] L. Serrao, S. Onori, and G. Rizzoni, "Ecms as a realization of pontryagin's minimum principle for hev control," in *Proceedings of the American Control Conference*, 2009, pp. 3964–3969.

[6] L. Serrao, S. Onori, A. Sciarretta, Y. Guezennec, and G. Rizzoni, "Optimal energy management of hybrid electric vehicles including battery aging," in *American Control Conference*, 2011, pp. 2125–2130.

[7] S. Ebbesen, P. Elbert, and L. Guzzella, "Battery state-of-health perceptive energy management for hybrid electric vehicles," *Vehicular Technology, IEEE Transactions on*, vol. 61, no. 7, pp. 2893–2900, 2012.

[8] S. Moura, J. Stein, and H. Fathy, "Battery-health conscious power management in plug-in hybrid electric vehicles via electrochemical modeling and stochastic control," *Control Systems Technology, IEEE Transactions on*, vol. 21, no. 3, pp. 679–694, 2013.

[9] T. M. Padovani, M. Debert, G. Colin, and Y. Chamaillard, "Optimal energy management strategy including battery health through thermal management for hybrid vehicles," in *Proceedings of 7th IFAC Symposium on Advances in Automotive Control*, 2013, pp. 384–389.

[10] M. Broussely, P. Biensan, F. Bonhomme, P. Blanchard, S. Herreyre, K. Nechev, and R. Staniewicz, "Main aging mechanisms in li ion batteries," *Journal of Power Sources*, vol. 146, no. 1-2, pp. 90 – 96, 2005.

[11] J. Vetter, P. Novák, M. Wagner, C. Veit, K.-C. Möller, J. Besenhard, M. Winter, M. Wohlfahrt-Mehrens, C. Vogler, and A. Hammouche, "Ageing mechanisms in lithium-ion batteries," *Journal of Power Sources*, vol. 147, no. 1-2, pp. 269–281, 2005.

[12] V. Agubra and J. Fergus, "Lithium ion battery anode aging mechanisms," *Materials*, vol. 6, no. 4, pp. 1310–1325, 2013.

[13] J. Zhang, B. Lu, Y. Song, and X. Ji, "Diffusion induced stress in layered li-ion battery electrode plates," *Journal of Power Sources*, vol. 209, no. 0, pp. 220 – 227, 2012.

[14] R. Kostecki and F. McLarnon, "Microprobe study of the effect of li intercalation on the structure of graphite," *Journal of Power Sources*, vol. 119-121, no. 0, pp. 550–554, 2003.

[15] J. Christensen and J. Newman, "Stress generation and fracture in lithium insertion materials," *Journal of Solid State Electrochemistry*, vol. 10, no. 5, pp. 293–319, 2006.

[16] J. Cho, Y. J. Kim, T.-J. Kim, and B. Park, "Zero-strain intercalation cathode for rechargeable li-ion cell," *Angewandte Chemie*, vol. 113, no. 18, pp. 3471–3473, 2001.

[17] J. B. Siegel, A. G. Stefanopoulou, P. Hagans, Y. Ding, and D. Gorsich, "Expansion of lithium ion pouch cell batteries: Observations from neutron imaging," *Journal of The Electrochemical Society*, vol. 160, no. 8, pp. A1031–A1038, 2013.

[18] J. Cannarella and C. B. Arnold, "Stress evolution and capacity fade in constrained lithium-ion pouch cells," *Journal of Power Sources*, vol. 245, no. 0, pp. 745–751, 2014.

[19] W. H. Woodford, W. C. Carter, and Y.-M. Chiang, "Design criteria for electrochemical shock resistant battery electrodes," *Energy Environ. Sci.*, vol. 5, pp. 8014–8024, 2012.

[20] R. Yazami and Y. Reynier, "Thermodynamics and crystal structure anomalies in lithium-intercalated graphite," *Journal of Power Sources*, vol. 153, no. 2, pp. 312–318, 2006.

[21] S. G. Stewart, V. Srinivasan, and J. Newman, "Modeling the performance of lithium-ion batteries and capacitors during hybrid-electric-vehicle operation," *Journal of The Electrochemical Society*, vol. 155, no. 9, pp. A664–A671, 2008.

[22] S. Di Cairano, W. Liang, I. V. Kolmanovsky, M. L. Kuang, and A. M. Phillips, "Power smoothing energy management and its application to a series hybrid powertrain," *Control Systems Technology, IEEE Transactions on*, vol. 21, no. 6, pp. 2091–2103, 2012.

[23] R. Bellman, *Dynamic Programming*. New York: Courier Dover Publications, 2003.

[24] O. Sundström and L. Guzzella, "A generic dynamic programming matlab function," in *Proceedings of the IEEE Control Applications & Intelligent Control*, 2009, pp. 1625–1630.

[25] J. C. Forman, S. Moura, J. Stein, and H. Fathy, "Optimal experimental design for modeling battery degradation," in *ASME Dynamic Systems Control Conference*, Fort Lauderdale, Florida, USA, Oct 17-19 2012.